Desalination and Water Treatment
www.deswater.com

doi: 10.5004/dwt.2017.21426

90 (2017) 262–272
September

Preparation and characterization of kaolin coated with Fe_3O_4 nanoparticles for the removal of hexavalent chromium: kinetic, equilibrium and thermodynamic studies

Azita Mohagheghian[a,b], Melina Pourmohseni[b], Robabeh Vahidi-Kolur[b], Jae-Kyu Yang[c], Mehdi Shirzad-Siboni[a,b,d,*]

[a]*Research Center of Health and Environment, Guilan University of Medical Sciences, Rasht, Iran*
[b]*Department of Environmental Health Engineering, School of Health, Guilan University of Medical Sciences, Rasht, Iran, Tel. +98 9111309440; email: mohagheghian@yahoo.com (A. Mohagheghian), Tel. +98 9117390924; email: melina.mohseni80@gmail.com (M. Pourmohseni), Tel. +98 9111850017; email: rvahidikolur@yahoo.com (R. Vahidi-Kolur)*
[c]*Ingenium College of Liberal Arts, Kwangwoon University, Seoul, Korea, Tel. +82 2 940 5769; email: jkyang@kw.ac.kr*
[d]*Department of Environmental Health Engineering, School of Public Health, Iran University of Medical Sciences, Tehran, Iran, Tel. +98 9112346428; Fax: +98 1333849413; emails: mshirzadsiboni@yahoo.com, mshirzadsiboni@gums.ac.ir (M. Shirzad-Siboni)*

Received 30 March 2017; Accepted 8 September 2017

ABSTRACT

In this study, removal of Cr(VI) by kaolin-Fe_3O_4 nanoparticles was investigated with variation of pH, adsorbent dosage, initial Cr(VI) concentration, ionic strength and temperature. Kaolin nanoparticles were synthesized by co-precipitation method. Maximum adsorption was observed at pH 3. The removal efficiency of Cr(VI) was increased with increasing adsorbent dosage, but was decreased with increasing initial Cr(VI) concentration and temperature. The removal efficiency of Cr(VI) was decreased in the presence of sulfate, chloride and bicarbonate ions while it was increased in the presence of carbonate ion. Studies of kinetic models and adsorption equilibrium revealed that the adsorption of Cr(VI) onto kaolin-Fe_3O_4 nanoparticles followed pseudo-second-order kinetic model and Freundlich isotherm. Maximum adsorption capacity was estimated to be 76.62 mg/g. Thermodynamic studies indicated that the adsorption of Cr(VI) onto kaolin-Fe_3O_4 nanoparticles was an exothermic (ΔH = –99.35 kJ/mol) process. Adsorption activity of Cr(VI) by kaolin-Fe_3O_4 nanoparticles was decreased (10%–30%) after 10 successive cycles.

Keywords: Kaolin-Fe_3O_4; Kinetic and isotherm models; Thermodynamics; Adsorption; Cr(VI)

1. Introduction

Chromium is a kind of toxic heavy metal and poses serious health problems by acting as a carcinogen, mutagen and teratogen in biological systems [1–3]. Chromium contamination in aquatic systems generally occurs through discharge of concentrated effluents from leather tanning, smelting, electroplating, paint, textile and paper industries [1,4–6]. Chromium is gradually accumulated in the living organisms and thereby causes life threatening diseases. Inorganic chromium is generally present as Cr(VI) and Cr(III) [4,7–9]. As Cr(VI) is more toxic and mobile than Cr(III), Cr(VI) contamination in aquatic environment is a great concern [1,4,10]. It is harmful to human health even at very low concentrations and has been categorized as a group I human carcinogen by the International Agency for Research on Cancer [1,4]. World Health Organization recommended 0.05 mg/L of Cr(VI) as a maximum allowable concentration in drinking water; while US Environmental Protection Agency has set 0.1 mg/L of Cr(VI) as a maximum contamination level [11]. Due to its toxicity, carcinogenicity and harmful property, removal of Cr(VI) from water system is very crucial [12,13]. Several physicochemical technologies such as ion exchange, electrocoagulation, reduction and adsorption have

* Corresponding author.

been used to treat wastewater contaminated with chromium [14–19]. Among them adsorption technique has much attention because it is simple, efficient and requires low operating cost [16,20]. Even though activated carbon has been widely used as an efficient adsorbent, it has limitation in large-scale application due to the relatively high preparation cost [20]. To compensate this limitation, several recycled adsorbents such as sawdust, agricultural residues, activated red mud, fly ash, dolomite, oyster shell, activated sludge, furnace slag, chitosan and kaolin have been applied to treat wastewater as low-cost adsorbents [21–27]. Kaolin has an aluminosilicate composition, which consists of stacked pairs of tetrahedral SiO_2 and octahedral Al_2O_3 sheets, with crystalline structure [28,29]. It has high adsorption capacity for several heavy metal ions and can be used as a supporting material due to its large surface area and pore volume [28,29]. When adsorption capacity of adsorbents has been exhausted, they should be separated from reaction systems [20,21]. In order to overcome this limitation, magnetic separation has much attention because it produces no contaminants and can treat large amount of wastewater within a short span of time [30–32]. Fe_3O_4 is a traditional magnetic material having superparamagnetic property. It can be recovered very quickly by external magnetic field and can be reused without losing its active sites [31–34]. Hence, the kaolin particles combined with Fe_3O_4 can be used as a promising adsorbent instead of the traditional adsorbents for large-scale wastewater treatment processes. A number of studies have been reported for the removal of Cr(VI) with kaolin alone [26,28,35]. Also there are many reports about removal of Cr(VI) with magnetite alone and magnetite nanocomposite [30,36,37]. However, limited information is available for the removal efficiency and removal kinetics of Cr(VI) with a natural adsorbent magnetized with Fe_3O_4 in the presence of different background electrolytes.

In this study, kaolin was magnetized by coating with the magnetite nanoparticles. This kaolin-Fe_3O_4 nanoparticles were used for the adsorption of Cr(VI) from aqueous solutions. The effects of pH, adsorbent dosage, initial Cr(VI) concentration, background electrolytes and temperature on the removal efficiency of Cr(VI) were studied. Adsorption kinetics, isotherm and thermodynamic studies were undertaken to elucidate adsorption mechanism and maximum adsorption capacity of kaolin-Fe_3O_4 nanoparticles.

2. Materials and methods

2.1. Chemicals

Iron(III) chloride ($FeCl_3.6H_2O$), iron(II) chloride ($FeCl_2.4H_2O$), $K_2Cr_2O_7$, 1,5-diphenylcarbazide, sodium hydroxide, sodium chloride, sodium sulphate, sodium hydrogen carbonate, sodium carbonate and hydrochloric acid were purchased from Merck (Germany) and used without any purification. Kaolin powder was obtained from Ideal Trades Men Company in Qazvin city from Iran. It was washed with deionized water, dried at 103°C for 3 h in an oven and then was sieved with 50 mesh ASTM. The main composition was SiO_2 (46.13%), Al_2O_3 (26.98%) and K_2O (2%) according to the above company. Stock solution (1,000 mg/L) of Cr(VI) was prepared by dissolving $K_2Cr_2O_7$ into distilled water and kept in a refrigerator. Initial pH of the solution was adjusted by addition of 0.1 M NaOH or HCl, and was measured by a pH meter (Metron, Switzerland). The experiments were carried out at room temperature (25°C ± 2°C).

2.2. Magnetization of the kaolin-Fe_3O_4 nanoparticles

Kaolin-Fe_3O_4 nanoparticles were prepared via a co-precipitation method in alkaline solution [32]. An appropriate amount of $FeCl_3.6H_2O$ and $FeCl_2.4H_2O$ was dissolved in 200 mL deionized water. Kaolin was added to the suspension at 1:1 volume ratio. 25 mL of NH_4OH solution (25%) was added drop-wise to the precursor solution to obtain an alkaline medium (pH = 8) producing a black and gelatinous precipitate of kaolin-Fe_3O_4 nanoparticles under nitrogen gas. It was heated at 80°C for 2 h with continuous stirring. The desired kaolin-Fe_3O_4 nanoparticles were collected by a permanent magnet and then were washed five times with distilled water and ethanol in order to remove any impurity. Then it was dried at 80°C in vacuum condition for 5 h. Compared with the preparation process of activated carbon, the preparation process of kaolin-Fe_3O_4 nanoparticles is generally performed at a relatively much lower temperature, requiring low energy cost. In order to analyze surface functional groups on the adsorbents, Fourier transform infrared spectroscopy (FT-IR) spectra were recorded using a PerkinElmer (Germany) spectrometer. The spectra were collected over a range from 400 to 4,000 cm^{-1}. The X-ray diffraction (XRD) studies were performed with a Philips XRD instrument (Siemens D-5000, Germany) using Cu Kα radiation (λ = 1.5406 Å) over a wide angle range (2θ value 4°–70°) at 40 kV of accelerating voltage and at 30 mA of emission current. The surface morphology of kaolin, Fe_3O_4 and kaolin-Fe_3O_4 nanoparticles were obtained by a field emission scanning electron microscopy (Mira3, Tescan, Czech Republic). SEM images were further supported by energy dispersive X-ray (EDX) to provide purity, qualitative and quantitative information of specific elements in adsorbents. The magnetic property of kaolin-Fe_3O_4 nanoparticles was characterized by vibrating sample magnetometer (VSM, MDKFD, Iran). The point of zero charge (pH_{zpc}) was determined to investigate the surface charge of the adsorbents. The pH_{zpc} of kaolin-Fe_3O_4 nanoparticles was determined adopting the method previously used [32,38].

2.3. Adsorption experiments

Adsorption experiments were performed in a 1 L Erlenmeyer flask containing Cr(VI) solution (30 mg/L) and kaolin-Fe_3O_4 nanoparticles (3 g/L). The mixtures were continuously stirred (150 rpm) at room temperature up to 240 min. At specified time intervals, 5 mL solution was taken from the flask containing mixture and then kaolin-Fe_3O_4 nanoparticles were separated from the solution by permanent magnet. The residual concentration of Cr(VI) was measured with colorimetric method. 2 mL of 1,5-diphenylcarbazide solution (0.25 g of 1,5-diphenylcarbazide was dissolved in 50 mL acetone) was added to each sample solution to form a complex and then it was measured using a UV/Visible spectrophotometer (Hach DR 5000, USA) at λ_{max} of 540 nm [34]. In order to study effects of various parameters, experiments were conducted at different amounts of adsorbent (0.25–3 g/L), initial Cr(VI) concentrations (5–50 mg/L), initial pH (3–11) and

temperature (298–323 K). The adsorption capacity of Cr(VI) by kaolin-Fe_3O_4 nanoparticles and removal efficiency were calculated by Eqs. (1) and (2), respectively [21]:

$$q = \frac{(C_0 - C_e)V}{M} \quad (1)$$

$$\text{Removal efficiency}(\%) = \frac{(C_0 - C_i)}{C_0} \times 100 \quad (2)$$

where q is the adsorption capacity (mg/g), C_0, C_i and C_e are initial, outlet and equilibrium concentrations of Cr(VI) (mg/L), V is the volume of Cr(VI) solution (L) and M is the total amount of kaolin-Fe_3O_4 nanoparticles (g).

3. Results and discussion

3.1. Adsorbent characterization

3.1.1. SEM, EDX and VSM analysis

SEM images of kaolin, Fe_3O_4 and kaolin-Fe_3O_4 nanoparticles are shown in Figs. 1(a)–(c), respectively. Fig. 1(c) clearly shows the distribution of magnetite nanoparticles on the surface of the kaolin. The particle size of Fe_3O_4 nanoparticles was around 20 nm. EDX microanalysis was used to characterize elemental composition of the Fe_3O_4 and kaolin-Fe_3O_4 nanoparticles. According to the EDX analysis, the major elements were Fe, O, Al, Si, K and Fe, indicating combination between kaolin and Fe_3O_4 nanoparticles [39]. VSM was used to measure magnetic property of Fe_3O_4 and kaolin-Fe_3O_4 nanoparticles. The saturated magnetization value of Fe_3O_4 and kaolin-Fe_3O_4 nanoparticles was 58.97 and 36.83 emu/g, respectively [39]. These results also indicated that the kaolin-Fe_3O_4 nanoparticles showed an excellent magnetic response to a magnetic field. Therefore, it can be separated easily and rapidly due to this high magnetic susceptibility. To identify crystal structure, mean crystal size, phase purity and functional groups on the surface of kaolin-Fe_3O_4 nanoparticles, were measured by X-ray diffraction (XRD) and Fourier transform infrared (FT-IR) spectrophotometer. XRD and FT-IR analysis also supported coating of Fe_3O_4 nanoparticles onto kaolin (data shown in our previous work) [39].

3.2. Effect of parameters on the removal of Cr(VI) with kaolin-Fe_3O_4 nanoparticles

3.2.1. The effect of solution pH

The effect of solution pH on the Cr(VI) (30 mg/L) adsorption onto kaolin-Fe_3O_4 nanoparticles (3 g/L) was investigated between pH 3–11 and the results are depicted in Fig. 2(a). Kaolin-Fe_3O_4 nanoparticles were not stable in strong acidic condition below pH 3. Considering the stability of the kaolin-Fe_3O_4 nanoparticles, adsorption experiments were performed between pH 3–11 in this work. Solution pH is recognized as one of the important parameters that governs the adsorption process. Fig. 2(a) shows that removal efficiency decreased by increasing the solution pH. Indeed, the removal efficiency decreased from 80.43% to 28.8% by increasing the solution pH from 3 to 11. Adsorption capacity decreased from 12.06 to 4.32 mg/g when the solution pH increased from 3 to 11 (Fig. 2(a)). Generally, surface charge of the adsorbents and

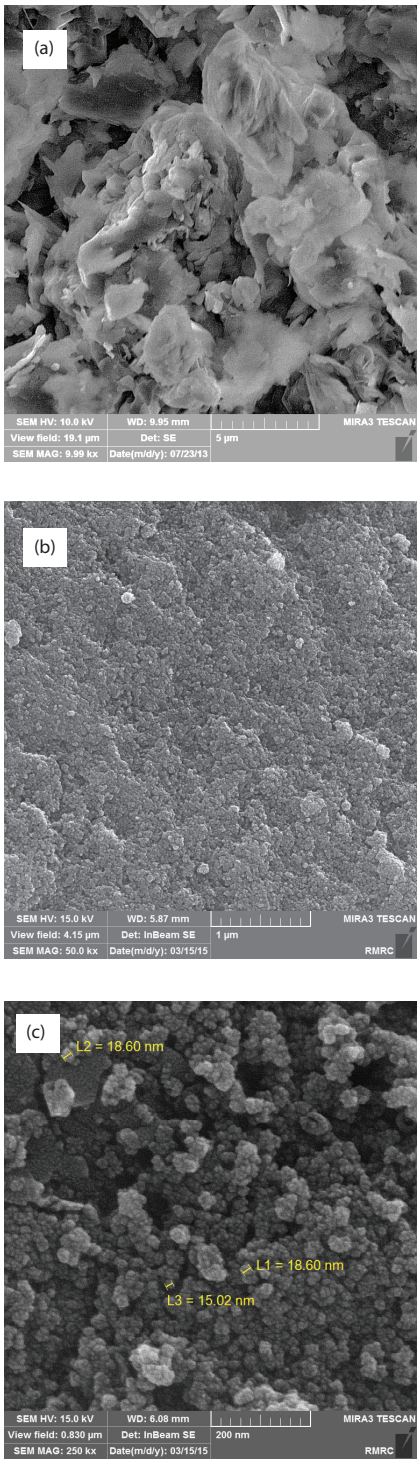

Fig. 1. SEM image of samples (a) kaolin, (b) Fe_3O_4 nanoparticles, (c) kaolin-Fe_3O_4 nanoparticles.

speciation of ionic contaminants is variable with variation of solution pH. Maximum removal efficiency was observed at pH 3. Indeed, the removal efficiency enhanced from 14.87% to 80.43% by increasing the reaction time from 2 to 240 min at pH 3. The favorable removal of Cr(VI) at lower pH can be explained by an anionic-type adsorption of Cr(VI) onto

kaolin-Fe_3O_4 nanoparticles as shown in Fig. 2(a). At low pH (pH 3), the dominant form of Cr(VI) is $HCrO_4^-$ and surface of the adsorbent is positively charged. But the $HCrO_4^-$ species is changed to more negative species such as CrO_4^{2-} and $Cr_2O_7^{2-}$ by increasing the pH from simulation of the Cr(VI) speciation using a MINTEQA2 program [21,27]. The decreased adsorption of Cr(VI) by increasing the pH may be due to the competition between CrO_4^{2-} and OH^- [21,27]. Similar observations have also been reported from other research groups [1,40,41]. The decreased adsorption of Cr(VI) with increasing pH also can be explained by the pH_{zpc} value of kaolin-Fe_3O_4 nanoparticles. According to the data, the pH_{zpc} of Fe_3O_4 and kaolin-Fe_3O_4 nanoparticles are 6 and 6.66, respectively (Fig. 2(b)). The pH_{zpc} for kaolin was reported as 7 [42]. On the other hand, the kaolin-Fe_3O_4 nanoparticles acquire a negative surface charge above this pH since the pH_{zpc} of kaolin-Fe_3O_4 nanoparticles is 6.66. At a pH lower than $pH_{zpc,}$ the surface of kaolin-Fe_3O_4 nanoparticles acquires positive charge and Cr(VI) molecules also has less negative charge [29]. Since the most effective removal of Cr(VI) was observed at pH 3, further experiments were performed at this pH.

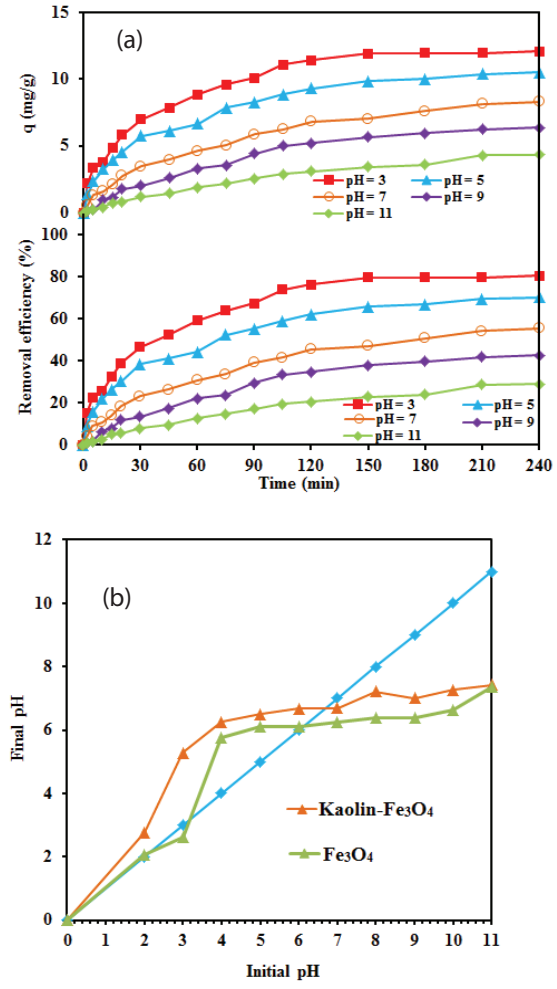

Fig. 2. (a) The effect of pH on the removal of Cr(VI) by kaolin-Fe_3O_4 nanoparticles in different time interval (initial Cr(VI) concentration = 30 mg/L, adsorbent dose = 2 g/L, 298 K) and (b) determination of the pH of point of zero charge (pH_{zpc}).

3.2.2. Effect of adsorbent dosage and reaction time

The influence of adsorbent dosage on the removal efficiency for Cr(VI) was investigated at various amounts of kaolin-Fe_3O_4 nanoparticles in the range of 0.25–3 g/L at pH 3. Indeed, the removal efficiency increased from 26.6% to 94.93% by increasing the adsorbent dosage from 0.25 to 3 g/L over the entire reaction time (2–240 min). This trend can be explained by the increased active sites along with the increase of the adsorbent dosage. The removal rate of Cr(VI) at all dosages was rapid in the first stages of reaction time (105 min) and then it was gradually slowed until reactions reach a near equilibrium after 240 min. The rapid adsorption at initial reaction time may be attributed to the abundance of free active sites on the surface of kaolin-Fe_3O_4 nanoparticles and easy availability of them for Cr(VI) molecules. As the active sites are occupied by Cr(VI), adsorption rates are decreased due to having little available active sites on the adsorbents [12,43]. Indeed, the removal efficiency enhanced from 25.72% to 94.93% by increasing the reaction time from 2 to 240 min at pH 3 with 3 g/L adsorbent. Since the most effective removal (%) of Cr(VI) was observed with adsorbent dosage equal to 3 g/L, the other experiments were performed at this adsorbent dosage.

3.2.3. The effect of initial Cr(VI) concentration

Removal efficiency of Cr(VI) was studied by varying the initial Cr(VI) concentration from 5 to 50 mg/L at constant adsorbent dosage (3 g/L) and at pH 3 (Fig. 3). When the initial Cr(VI) concentration was increased from 5 to 50 mg/L, the Cr(VI) removal efficiency was decreased from 99.99% to 71.72%. This result can be explained by the fact that the adsorbent has a limited number of active sites, which would become saturated above a certain Cr(VI) concentration [12,43]. Nevertheless, the adsorption capacity increased from 1.66 to 17.93 mg/g when the initial Cr(VI) concentration increased from 5 to 50 mg/L (Fig. 3).

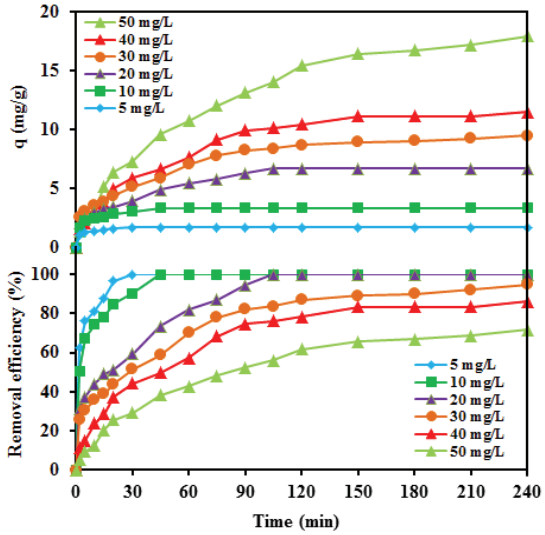

Fig. 3. Effect of initial Cr(VI) concentration on the removal of Cr(VI) by kaolin-Fe_3O_4 nanoparticles in different time interval (pH = 3, adsorbent dose = 3 g/L, 298 K).

3.2.4. Effect of the presence of different ions on removal of Cr(VI)

There are various kinds of anions, such as chloride, sulfate, carbonate and bicarbonate in water and wastewater, causing positive or negative effects on Cr(VI) adsorption. To assess the effect of different type of anions such as Cl^-, CO_3^{2-}, HCO_3^- and SO_4^{2-} on the removal efficiency of Cr(VI), constant concentrations of NaCl, Na_2CO_3, $NaHCO_3$ and Na_2SO_4 (30 mg/L) were added to the reactor in the optimal conditions (initial Cr(VI) concentration 30 mg/L, adsorbent dosage (3 g/L) and pH 3) before beginning the adsorption (Fig. 4). The removal efficiency of Cr(VI) was decreased in the presence of sulfate (84.66%), chloride (91.52%) and bicarbonate (93.99%) ions but was increased in the presence of carbonate (95.31%) ion. Fig. 4 shows that removal efficiency of Cr(VI) was decreased in the presence of Cl^-, HCO_3^- and SO_4^{2-}. However, it was difficult to clearly explain the decreased removal of Cr(VI) in the presence of three background electrolytes in this work.

3.2.5. Comparison of each process and desorption efficiency

Removal efficiency of Cr(VI) by kaolin, Fe_3O_4 and kaolin-Fe_3O_4 nanoparticles were compared at 30 mg/L Cr(VI) concentration, at 3 g/L adsorbent dosage and at pH 3. Fig. 5 shows that removal efficiency for each process was 23.74%, 56.55% and 94.93%. These experiments demonstrate that both kaolin and Fe_3O_4 nanoparticles are necessary for the effective removal of Cr(VI). Reusability of adsorbent is an important factor for the application of developed adsorbent in the treatment of wastewater. Hence, desorption of Cr(VI) from the surface was performed using three different washing solutions such as deionized water, 0.1 M NaOH and HNO_3. The adsorption and desorption process was performed for 10 repeated runs. The removal efficiency at each run was Run 1 (94.93%) as control, Run 2 (73.38%), Run 3 (65.69%), Run 4 (59.92%) washing with deionized water, Run 5 (78.23%), Run 6 (78.54.2%), Run 7 (76.02%) washing with 0.1 M NaOH, Run 8 (68.06%), Run 9 (76.63%) and Run 10 (59.22%) washing with 0.1 M HNO_3. As can be seen in Fig. 6, adsorption capacity of Cr(VI) by kaolin-Fe_3O_4 nanoparticles was maintained up to 10 consecutive runs, suggesting a plausible adsorbent in the treatment of Cr(VI) from water and wastewater.

3.3. Kinetic, equilibrium and thermodynamic studies

Adsorption kinetic experiments were performed at different Cr(VI) concentration (5–50 mg/L), at constant adsorbent dosage (3 g/L) and at pH 3. The pseudo-first-order,

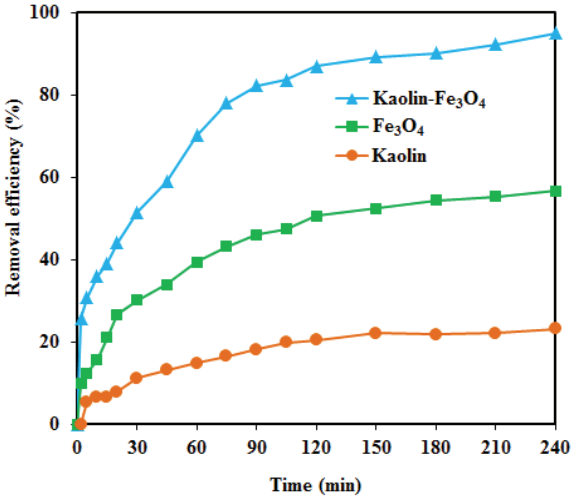

Fig. 5. Removal of Cr(VI) by different process in different time interval (pH = 3, initial Cr(VI) concentration = 30 mg/L, adsorbent dose = 3 g/L, 298 K).

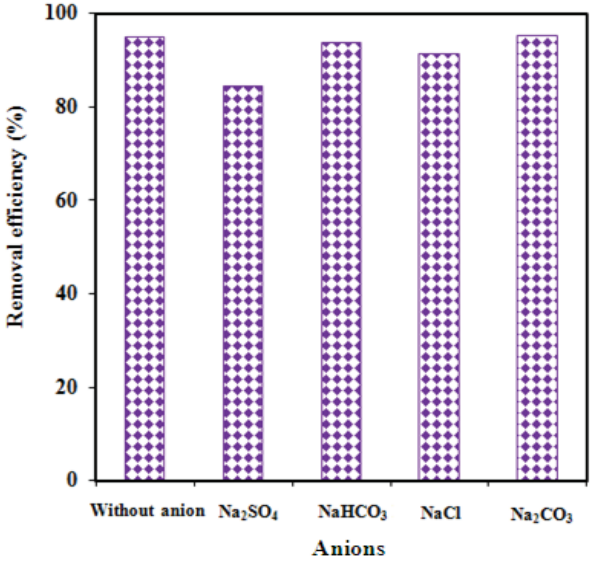

Fig. 4. Effect of the presence of different ions on the removal of Cr(VI) by kaolin-Fe_3O_4 nanoparticles (pH = 3, initial Cr(VI) concentration = 30 mg/L, adsorbent dose = 3 g/L, 298 K).

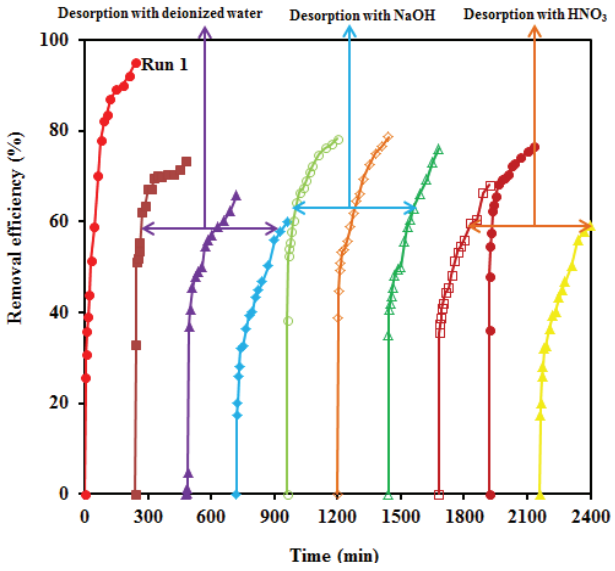

Fig. 6. The results of reusability test of kaolin-Fe_3O_4 nanoparticles in different time interval (pH = 3, initial Cr(VI) concentration = 30 mg/L, adsorbent dose = 3 g/L, 298 K).

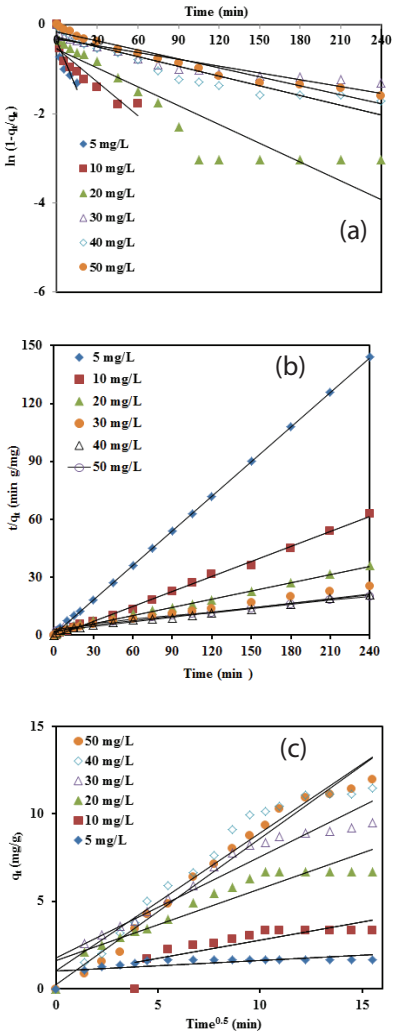

Fig. 7. Linear plots of (a) pseudo-first-order (b) pseudo-second-order and (c) intra-particle diffusion models for the removal of Cr(VI) by kaolin-Fe_3O_4 nanoparticles (pH = 3, initial Cr(VI) concentration = 30 mg/L, adsorbent dose = 3 g/L, 298 K).

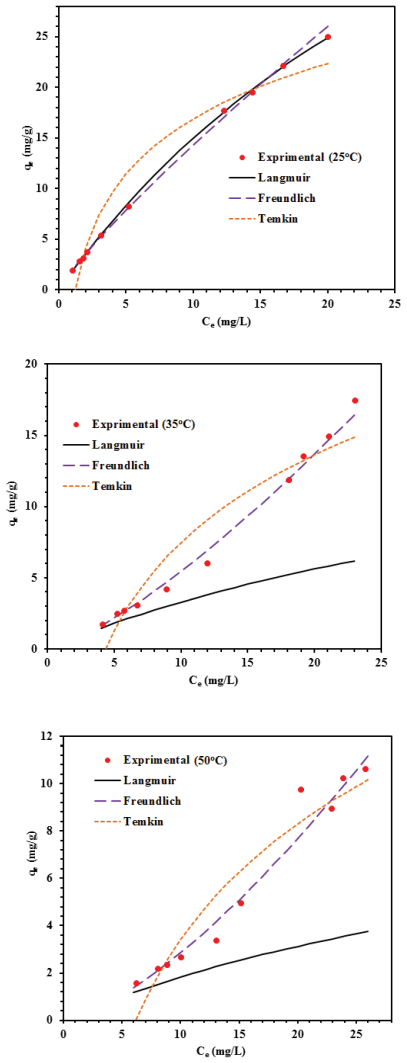

Fig. 8. Comparison of different isotherm models for Cr(VI) adsorption onto kaolin-Fe_3O_4 nanoparticles at different temperature (pH = 3, initial Cr(VI) concentration = 30 mg/L).

pseudo-second-order and intra-particle diffusion models were applied in order to find an efficient model for the description of adsorption. The relevant equations for the kinetic, equilibrium and thermodynamic studies are shown in Table 1 [44–49]. To obtain kinetic data for the removal of Cr(VI), $\ln\left(1-\frac{q_t}{q_e}\right)$ vs. t, $\frac{t}{q_t}$ vs. t, and q_t vs. $t^{0.5}$ was plotted for the pseudo-first-order, pseudo-second-order and intra-particle diffusion models, respectively (Figs. 7(a)–(c)). The kinetic parameters for the removal Cr(VI) at different initial Cr(VI) concentrations and pH are summarized in Tables 2 and 3, respectively. The kinetic data for Cr(VI) adsorption showed the best fitting (R^2 = 0.9897) with the pseudo-second-order model. Moreover, when the initial Cr(VI) concentration increased from 5 to 50 mg/L, the value of k_2 (g/mg min) and R^2 for the pseudo-second-order model were decreased from 1.085 to 0.024 g/mg min and 0.999 to 0.9709, respectively. Also, q_e (mg/g) was increased from 1.679 to 13.605 mg/g. This result indicated that adsorption data was in agreement with

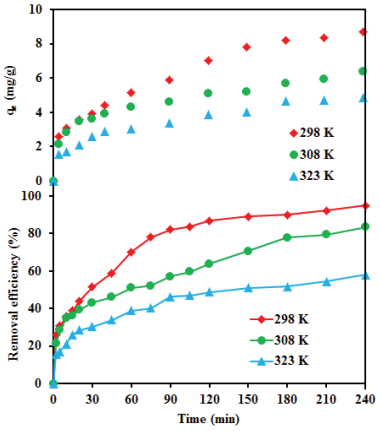

Fig. 9. The effect of temperature on the removal of Cr(VI) by kaolin-Fe_3O_4 nanoparticles in different time interval (pH = 3, initial Cr(VI) concentration = 30 mg/L, adsorbent dose = 3 g/L).

Table 1
The kinetic, isotherm and thermodynamic equations for adsorption of Cr(VI) onto kaolin-Fe_3O_4 nanoparticles

Kinetic models	Isotherm equations	Thermodynamic equations
Pseudo-first-order	Freundlich isotherm	Van't Hoff
$\ln\left(1-\frac{q_t}{q_e}\right)=-k_1t$	$\log q_e=\log K_F+\frac{1}{n}\log C_e$	$\ln(K_l)=\frac{\Delta S}{R}-\frac{\Delta H}{RT}$
Pseudo-second-order	Langmuir isotherm	Free energy of adsorption
$\frac{t}{q_t}=\frac{1}{k_2{q_e}^2}+\frac{1}{q_e}t$	$q_e=\frac{K_Lq_mC_e}{1+K_LC_e}$	$\Delta G=-RT\ln K_L$
Intra-particle diffusion model	Temkin isotherm	
$q_t=K_p\times t^{0.5}+C$	$q_e=B\ln K_t+B\ln C_e$	
	Separation factor (R_L)	
	$R_L=\frac{1}{1+K_LC_0}$	

Parameters: q_e (mg/g), q_t (mg/g), k_1 (1/min), k_2 (g/mg min), K_L (L/mg), q_m (mg/g), K_F (mg/g (L mg)$^{1/n}$), K_p (mg/g min$^{-0.5}$), C_0 (mg/g), $B = RT/bt$, K_t (L/g), b_t (J/mol), ΔS (J/mol K), ΔH (kJ/mol), R (8.314 J/mol K), T (K).

Table 2
The calculated kinetic parameters for pseudo-first-order, pseudo-second-order and intra-particle diffusion models for removal of Cr(VI) with kaolin-Fe_3O_4 nanoparticles (pH = 3, adsorbent dose = 3 g/L, 298 K)

$[Cr(VI)]_0$ (mg/L)	q_e(exp) (mg/g)	Pseudo-first-order model			Pseudo-second-order model			Intra-particle diffusion model		
		k_1 (1/min)	q_e (cal) (mg/g)	R^2	k_2 (g/mg min)	q_e (exp) (mg/g)	R^2	K_p (mg/g min$^{-0.5}$)	C_0 (mg/g)	R^2
5	1.66	0.0721	2	0.7318	1.085	1.676	0.9999	0.0584	1.0288	0.4339
10	3.33	0.0252	4	0.8127	0.411	3.865	0.9979	0.02061	0.7266	0.6555
20	6.66	0.014	7	0.8385	0.0755	7.107	0.9932	0.4095	1.607	0.8821
30	9.49	0.005	13	0.8596	0.054	9.49	0.9897	0.5811	1.7442	0.9296
40	11.46	0.0073	14	0.8937	0.0377	12.61	0.9851	0.791	1.0119	0.9428
50	11.95	0.0067	15	0.9533	0.024	13.605	0.9709	0.8479	0.2042	0.9762

Table 3
The calculated kinetic parameters for pseudo-first-order and pseudo-second-order models for removal of Cr(VI) with kaolin-Fe_3O_4 nanoparticles at different pHs (initial Cr(VI) concentration = 30 mg/L, adsorbent dose = 2 g/L, 298 K)

pH	q_e(exp) (mg/g)	Pseudo-first-order model			Pseudo-second-order model		
		k_1 (1/min)	q_e (cal) (mg/g)	R^2	k_2 (g/mg min)	q_e (exp) (mg/g)	R^2
3	12.064	0.085	14	0.8987	0.0497	13.037	0.99
5	10.51	0.0127	11	0.9894	0.0388	11.35	0.9839
7	8.29	0.0102	9	0.9937	0.0227	9.345	0.9596
9	3.37	0.0071	8	0.976	0.0092	9.469	0.785
11	4.32	0.0082	5	0.9828	0.00085	6.142	0.843

Table 4
The calculated isotherm and thermodynamic parameters for removal of Cr(VI) with kaolin-Fe_3O_4 nanoparticles

Freundlich model				Langmuir model			Temkin model			Thermodynamic parameters		
T (K)	K_F (mg/g (L mg)$^{1/n}$)	n	R^2	q_m (mg/g)	K_L (L/mg)	R^2	K_t (L/g)	b_t (J/mol)	R^2	ΔG (kJ/mol)	ΔH (kJ/mol)[a]	ΔS (J/mol K)
298	1.95	1.155	0.9992	76.62	0.025	0.9693	1.18	313.4	0.948	9.13	–99.35	–53.97
308	3.894	0.753	0.9935	18.93	0.021	0.9618	4.31	288.06	0.913	9.89	–	–
323	9.382	0.55	0.9766	10.845	0.02	0.8441	6.16	380.775	0.9115	10.5	–	–

[a]Results of plotting $\ln K_L$ vs. $1/T$: slope = 826.05, intercept = 6.4918, R^2 = 0.8438.

Table 5
Comparison of monolayer adsorption capacity of Cr(VI) using different adsorbent

Temperature (K)	Adsorbent	Freundlich constants			Langmuir constants			Thermodynamic parameters			Reference
		K_F (mg/g (L mg)$^{1/n}$)	n	R^2	q_m (mg/g)	K_L (L/mg)	R^2	ΔG (kJ/mol)	ΔH (kJ/mol)	ΔS (J/mol K)	
303	Wollastonite	–	–	–	0.686	0.224	–	–13.65	1.72	36.42	[51]
313	Wollastonite	–	–	–	0.749	0.315	–	–14.94	2.09	5.44	[51]
323	Wollastonite	–	–	–	0.826	0.323	–	–15.53	–	–	[51]
303	Nonactivated kaolinite	1.1	0.4	0.96	11.6	0.032	0.99	–26.8	30.4	88.4	[52]
308	Nonactivated kaolinite	–	–	–	–	–	–	–27.2	–	–	[52]
313	Nonactivated kaolinite	–	–	–	–	–	–	–27.6	–	–	[52]
303	Acid-activated kaolinite	1.5	0.4	0.95	13.9	0.039	0.99	–59.9	63.9	198.1	[52]
308	Acid-activated kaolinite	–	–	–	–	–	–	–60.9	–	–	[52]
313	Acid-activated kaolinite	–	–	–	–	–	–	–61.9	–	–	[52]
303	ZrO-kaolinite	1	0.4	0.96	10.9	0.031	0.99	–26.5	30.5	87.8	[52]
308	ZrO-kaolinite	–	–	–	–	–	–	–27	–	–	[52]
313	ZrO-kaolinite	–	–	–	–	–	–	–27.5	–	–	[52]
303	Tetrabutylammonium kaolinite	0.9	0.4	0.97	10.6	0.029	0.99	–28	32.1	92.5	[52]
308	Tetrabutylammonium kaolinite	–	–	–	–	–	–	–28.4	–	–	[52]
313	Tetrabutylammonium kaolinite	–	–	–	–	–	–	–28.9	–	–	[52]
277	Spent activated clay	–	–	–	0.503	1.956	0.998	–28.86	25.31	196.648	[53]
287	Spent activated clay	–	–	–	0.518	2.397	0.999	–30.66	–	–	[53]
297	Spent activated clay	–	–	–	0.526	1.902	0.997	–32.92	–	–	[53]
313	Spent activated clay	–	–	–	0.557	6.185	0.991	–35.82	–	–	[53]
303	Fuller's earth	1.24	1.59	0.9938	23.58	0.037	0.9925	–6.50	–	–	[54]
298	Magnetic	2.94	3.62	0.991	3.55	7.578	0.996	–11.55	31.17	143.34	[55]
308	Magnetic	–	–	–	–	–	–	–12.97	–	–	[55]
318	Magnetic	–	–	–	–	–	–	–15.23	–	–	[55]
298	Montmorillonite-magnetite	1.62	2.63	0.984	13.88	0.030	0.965	–	–	–	[56]
298	Diatomite-magnetite	–	–	–	12.31	0.015	0.799	–	–	–	[57]
298	Fe_3O_4@n-SiO_2	1.70	23.26	0.93	2.66	4.90	0.98	–6.36	28.22	0.11	[37]
308	Fe_3O_4@n-SiO_2	1.85	13.38	0.99	2.79	6.74	0.98	–7.52	–	–	[37]
318	Fe_3O_4@n-SiO_2	1.89	15.13	0.99	3.78	10	0.94	–9.60	–	–	[37]
293	Ti-Fe kaolinite	11.12	0.209	0.991	23.47	1.078	0.993	–4.619	32.424	146.42	[58]
303	Ti-Fe kaolinite	–	–	–	–	–	–	–5.173	–	–	[58]
313	Ti-Fe kaolinite	–	–	–	–	–	–	–5.651	–	–	[58]
323	Ti-Fe kaolinite	–	–	–	–	–	–	–6.573	–	–	[58]
333	Ti-Fe kaolinite	–	–	–	–	–	–	–7.112	–	–	[58]

this model. The value of C was measured as 1.7442 mg/g, indicating that intra-particle diffusion is not the single controlling step for Cr(VI) adsorption and the process is also partially controlled by boundary layer diffusion.

To investigate adsorption equilibrium isotherm, experiments were performed with 30 mg/L Cr(VI) as an initial concentration using various adsorbent dosages (0.4–15 g/L) at pH 3 for 72 h. All experiments were repeated three times and average values were reported. Langmuir, Freundlich and Temkin equations were applied to fit experimental adsorption data, and the related equations are shown in Table 1 [50]. Different adsorption isotherms obtained at various temperatures are illustrated in Fig. 8. To obtain equilibrium data for the removal of Cr(VI), C_e/q_e vs. C_e, $\log q_e$ vs. $\log C_e$ and q_e vs. $\ln C_e$ was plotted for the Langmuir, Freundlich and Temkin models, respectively. The Langmuir, Freundlich and Temkin isotherm constants at different temperature are given in Table 4. The correlation coefficient R^2 = 0.9992, 0.9935 and 0.97666 at temperatures of 298, 303 and 323 K indicates that adsorption of the Cr(VI) onto the kaolin-Fe_3O_4 nanoparticles follows the Freundlich isotherm. The Freundlich adsorption heterogeneity factors (n values) were in the range of 1.155–0.55, at 293–323 K, indicating that Cr(VI) was favorably adsorbed by kaolin-Fe_3O_4 nanoparticles. R_L value (separation factor) expresses a characteristic of the Langmuir isotherm. Generally adsorption will be favorable when R_L value is between 0 and 1. But adsorption is unfavorable when R_L value is above 1. R_L value 1 and 0 means linear and irreversible adsorptions, respectively. Separation factor (R_L) at temperatures of 298, 303 and 323 K was calculated as 0.666–0.975, 0.674–0.92 and 0.66–0.889, respectively. The monolayer saturation capacity at 298, 303 and 323 K was 76.62, 18.93 and 10.845 mg/g, respectively.

Thermodynamic experiments were performed at different temperature from 298 to 323 K at constant adsorbent dosage (3 g/L) and at pH 3 (Fig. 9). When the temperature was increased from 298 to 323 K, the Cr(VI) removal efficiency was decreased from 94.93% to 58.04%. The related equations are shows in Table 1 [50]. From linear plot between $\ln K_L$ and $1/T$, ΔH (kJ mol^{-1}) and ΔS (J/mol K) were calculated from the slope and intercept, respectively. The values of ΔS, ΔH, ΔG and q_m at different temperature are given in Table 4. ΔH (kJ/mol) value was negative. It means that adsorption is favorable at low temperature. The removal capacity of Cr(VI) by kaolin-Fe_3O_4 nanoparticles was compared with that by other adsorbents in Table 5. Maximum adsorption capacity was obtained as 76.62 mg/g at pH 3. Based on the obtained results, the kaolin-Fe_3O_4 nanoparticles can be regarded as an efficient adsorbent for removal of Cr(VI) from water and wastewater.

4. Conclusions

Kaolin-Fe_3O_4 nanoparticles were used as an adsorbent for the removal of Cr(VI) in aqueous solution. Kaolin-Fe_3O_4 nanoparticles showed super paramagnetic property with 36.83 emu/g. The prepared adsorbent was characterized by SEM and VSM. Adsorption of Cr(VI) was dependent on initial Cr(VI) concentrations and solution pH. The removal efficiency was maximum at pH 3 and was increased with increasing reaction time and adsorption dosage, but was decreased with increasing initial Cr(VI) concentration and temperature. The pseudo-second-order model better described the adsorption data of Cr(VI) onto adsorbent than the pseudo-first-order model and the intra-particle diffusion model. When Freundlich, Langmuir and Temkin equations were used to fit the experimental isothermal data, experimental results were well fitted with the Freundlich equation. According to the obtained results, the maximum adsorption capacity of Cr(VI) by kaolin-Fe_3O_4 nanoparticles was 76.62 and 10.85 mg/g at 298 and 323 K, respectively. Considering the observed results such as a typical anionic-type adsorption behavior, favorable adsorption at low temperature, better fitting with Freundlich equation than Langmuir equation, decreased adsorption in the presence of different background electrolytes, we think that adsorption may occur through both an outer-sphere complexation and physical adsorption. The results indicate that kaolin-Fe_3O_4 nanoparticles are effective adsorbent for the removal of Cr(VI) from aqueous solutions.

Acknowledgments

The authors thank the Guilan and Iran Universities of Medical Sciences of Iran for their contributions.

References

[1] L.J. Yu, S.S. Shukla, K.L. Dorris, A. Shukla, J. Margrave, Adsorption of chromium from aqueous solutions by maple sawdust, J. Hazard. Mater., 100 (2003) 53–63.
[2] Z. Al-Othman, R. Ali, M. Naushad, Hexavalent chromium removal from aqueous medium by activated carbon prepared from peanut shell: adsorption kinetics, equilibrium and thermodynamic studies, Chem. Eng. J., 184 (2012) 238–247.
[3] A.A. Alqadami, M. Naushad, M.A. Abdalla, T. Ahamad, Z.A. AlOthman, S.M. Alshehri, A.A. Ghfar, Efficient removal of toxic metal ions from wastewater using a recyclable nanocomposite: a study of adsorption parameters and interaction mechanism, J. Cleaner Prod., 156 (2017) 426–436.
[4] S.A. Katz, H. Salem, The toxicology of chromium with respect to its chemical speciation: a review, J. Appl. Toxicol., 13 (1993) 217–224.
[5] M. Shirzad Siboni, M.-T. Samadi, J.-K. Yang, S.-M. Lee, Photocatalytic removal of Cr(VI) and Ni(II) by UV/TiO_2: kinetic study, Desal. Wat. Treat., 40 (2012) 77–83.
[6] A. Basumatary, P. Vikram Singh, R. Vinoth Kumar, A. Ghoshal, G. Pugazhenthi, Development and characterization of a MCM-48 ceramic composite membrane for the removal of Cr(VI) from an aqueous solution, J. Environ. Eng., 142 (2015) C4015013.
[7] M. Mahmoud, A. Yakout, H. Abdel-Aal, M. Osman, Speciation and selective biosorption of Cr(III) and Cr(VI) using nanosilica immobilized-fungi biosorbents, J. Environ. Eng., 141 (2014) 04014079.
[8] S. Rangabhashiyam, N. Selvaraju, B. Raj Mohan, P. Muhammed Anzil, K. Amith, E. Ushakumary, Hydrous cerium oxide nanoparticles impregnated Enteromorpha sp. for the removal of hexavalent chromium from aqueous solutions, J. Environ. Eng., 142 (2015) C4015016.
[9] G. Sharma, M. Naushad, A.H. Al-Muhtaseb, A. Kumar, M.R. Khan, S. Kalia, M. Bala, A. Sharma, Fabrication and characterization of chitosan-crosslinked-poly (alginic acid) nanohydrogel for adsorptive removal of Cr (VI) metal ion from aqueous medium, Int. J. Biol. Macromol., 95 (2017) 484–493.
[10] M. Shirzad Siboni, M.T. Samadi, J.K. Yang, S.M. Lee, Photocatalytic reduction of Cr(VI) and Ni(II) in aqueous solution by synthesized nanoparticle ZnO under ultraviolet light irradiation: a kinetic study, Environ. Technol., 32 (2011) 1573–1579.

[11] A.Z.M. Badruddoza, Z.B.Z. Shawon, M.T. Rahman, K.W. Hao, K. Hidajat, M.S. Uddin, Ionically modified magnetic nanomaterials for arsenic and chromium removal from water, Chem. Eng. J., 225 (2013) 607–615.
[12] S.P. Dubey, K. Gopal, Adsorption of chromium (VI) on low cost adsorbents derived from agricultural waste material: a comparative study, J. Hazard. Mater., 145 (2007) 465–470.
[13] Z.A. ALOthman, M. Naushad, R. Ali, Kinetic, equilibrium isotherm and thermodynamic studies of Cr (VI) adsorption onto low-cost adsorbent developed from peanut shell activated with phosphoric acid, Environ. Sci. Pollut. Res., 20 (2013) 3351–3365.
[14] S. Rengaraj, K.-H. Yeon, S.-H. Moon, Removal of chromium from water and wastewater by ion exchange resins, J. Hazard. Mater., 87 (2001) 273–287.
[15] T. Ölmez, The optimization of Cr (VI) reduction and removal by electrocoagulation using response surface methodology, J. Hazard. Mater., 162 (2009) 1371–1378.
[16] N. Daneshvar, D. Salari, S. Aber, Chromium adsorption and Cr (VI) reduction to trivalent chromium in aqueous solutions by soya cake, J. Hazard. Mater., 94 (2002) 49–61.
[17] M. Kobya, Removal of Cr(VI) from aqueous solutions by adsorption onto hazelnut shell activated carbon: kinetic and equilibrium studies, Bioresour. Technol., 91 (2004) 317–321.
[18] A. Bhattacharya, S. Mandal, S. Das, Removal of Cr (VI) from aqueous solution by adsorption onto low cost non-conventional adsorbents, Indian J. Chem. Technol., 13 (2006) 576–583.
[19] S. Goswami, U.C. Ghosh, Studies on adsorption behaviour of Cr (VI) onto synthetic hydrous stannic oxide, Water SA, 31 (2006) 597–602.
[20] K. Selvi, S. Pattabhi, K. Kadirvelu, Removal of Cr(VI) from aqueous solution by adsorption onto activated carbon, Bioresour. Technol., 80 (2001) 87–89.
[21] N.K. Hamadi, X.D. Chen, M.M. Farid, M.G.Q. Lu, Adsorption kinetics for the removal of chromium (VI) from aqueous solution by adsorbents derived from used tyres and sawdust, Chem. Eng. J., 84 (2001) 95–105.
[22] A. Bhattacharya, T. Naiya, S. Mandal, S. Das, Adsorption, kinetics and equilibrium studies on removal of Cr (VI) from aqueous solutions using different low-cost adsorbents, Chem. Eng. J., 137 (2008) 529–541.
[23] G. Shams Khorramabadi, R. Darvishi Cheshmeh Soltani, A. Rezaee, A.R. Khataee, A. Jonidi Jafari, Utilisation of immobilised activated sludge for the biosorption of chromium (VI), Can. J. Chem. Eng., 90 (2012) 1539–1546.
[24] E. Nehrenheim, J.P. Gustafsson, Kinetic sorption modelling of Cu, Ni, Zn, Pb and Cr ions to pine bark and blast furnace slag by using batch experiments, Bioresour. Technol., 99 (2008) 1571–1577.
[25] R. Schmuhl, H. Krieg, K. Keizer, Adsorption of Cu (II) and Cr (VI) ions by chitosan: kinetics and equilibrium studies, Water SA, 27 (2004) 1–8.
[26] V. Chantawong, N.W. Harvey, V.N. Bashkin, Comparison of heavy metal adsorptions by Thai kaolin and ballclay, Water Air Soil Pollut., 148 (2003) 111–125.
[27] M. Shirzad-Siboni, S. Azizian, S.M. Lee, The removal of hexavalent chromium from aqueous solutions using modified holly sawdust: equilibrium and kinetics studies, Environ. Eng. Res., 16 (2011) 55–60.
[28] C. Quintelas, Z. Rocha, B. Silva, B. Fonseca, H. Figueiredo, T. Tavares, Removal of Cd (II), Cr (VI), Fe (III) and Ni (II) from aqueous solutions by an *E. coli* biofilm supported on kaolin, Chem. Eng. J., 149 (2009) 319–324.
[29] M. Shirzad-Siboni, M. Farrokhi, R. Darvishi Cheshmeh Soltani, A. Khataee, S. Tajassosi, Photocatalytic reduction of hexavalent chromium over ZnO nanorods immobilized on kaolin, Ind. Eng. Chem. Res., 53 (2014) 1079–1087.
[30] R. Chen, L. Chai, Q. Li, Y. Shi, Y. Wang, A. Mohammad, Preparation and characterization of magnetic Fe_3O_4/CNT nanoparticles by RPO method to enhance the efficient removal of Cr (VI), Environ. Sci. Pollut. Res. Int., 20 (2013) 7175–7185.
[31] M. Farrokhi, S.-C. Hosseini, J.-K. Yang, M. Shirzad-Siboni, Application of ZnO–Fe_3O_4 nanocomposite on the removal of azo dye from aqueous solutions: kinetics and equilibrium studies, Water Air Soil Pollut., 225 (2014) 1–12.
[32] A. Mohagheghian, R. Vahidi-Kolur, M. Pourmohseni, J.-K. Yang, M. Shirzad-Siboni, Application of scallop shell-Fe_3O_4 nanocomposite for the removal azo dye from aqueous solutions, Water Air Soil Pollut., 226 (2015) 1–16.
[33] S. Abkenar, M. Khoobi, R. Tarasi, M. Hosseini, A. Shafiee, M. Ganjali, Fast removal of methylene blue from aqueous solution using magnetic-modified Fe_3O_4 nanoparticles, J. Environ. Eng., 141 (2014) 04014049.
[34] A.A. Alqadami, M. Naushad, M.A. Abdalla, T. Ahamad, Z.A. Alothman, S.M. Alshehri, Synthesis and characterization of Fe_3O_4@TSC nanocomposite: highly efficient removal of toxic metal ions from aqueous medium, RSC Adv., 6 (2016) 22679–22689.
[35] Y. Li, Q.-Y. Yue, B.-Y. Gao, Effect of humic acid on the Cr (VI) adsorption onto kaolin, Appl. Clay Sci., 48 (2010) 481–484.
[36] S. Luther, N. Brogfeld, J. Kim, J. Parsons, Study of the thermodynamics of chromium (III) and chromium (VI) binding to Fe_3O_4 and $MnFe_2O_4$ nanoparticles, J. Colloid Interface Sci., 400 (2013) 97.
[37] V. Srivastava, Y. Sharma, Synthesis and characterization of Fe_3O_4@ n-SiO_2 nanoparticles from an agrowaste material and its application for the removal of Cr (VI) from aqueous solutions, Water Air Soil Pollut., 225 (2014) 1–16.
[38] M. Shirzad-Siboni, A. Khataee, F. Vafaei, S.W. Joo, Comparative removal of two textile dyes from aqueous solution by adsorption onto marine-source waste shell: kinetic and isotherm studies, Korean J. Chem. Eng., 31 (2014) 1451–1459.
[39] A. Mohagheghiana, M. Pourmohsenia, R. Vahidi-Kolura, J.-K. Yangb, M. Shirzad-Siboni, Application of kaolin-Fe_3O_4 nanocomposite for the removal of azo dye from aqueous solutions, Desal. Wat. Treat., 58 (2017) 308–319.
[40] M.R. Unnithan, T. Anirudhan, The kinetics and thermodynamics of sorption of chromium (VI) onto the iron (III) complex of a carboxylated polyacrylamide-grafted sawdust, Ind. Eng. Chem. Res., 40 (2001) 2693–2701.
[41] F. Gode, E.D. Atalay, E. Pehlivan, Removal of Cr (VI) from aqueous solutions using modified red pine sawdust, J. Hazard. Mater., 152 (2008) 1201–1207.
[42] B. Nandi, A. Goswami, M. Purkait, Removal of cationic dyes from aqueous solutions by kaolin: kinetic and equilibrium studies, Appl. Clay Sci., 42 (2009) 583–590.
[43] B. Babu, S. Gupta, Adsorption of Cr (VI) using activated neem leaves: kinetic studies, Adsorption, 14 (2008) 85–92.
[44] S. Azizian, Kinetic models of sorption: a theoretical analysis, J. Colloid Interface Sci., 276 (2004) 47–52.
[45] M. Shirzad-Siboni, A. Khataee, S.W. Joo, Kinetics and equilibrium studies of removal of an azo dye from aqueous solution by adsorption onto scallop, J. Ind. Eng. Chem., 20 (2014) 610–615.
[46] M. Samarghandi, S. Azizian, M.S. Siboni, S. Jafari, S. Rahimi, Removal of divalent nickel from aqueous solutions by adsorption onto modified holly sawdust: equilibrium and kinetics, Iran. J. Environ. Health Sci. Eng., 8 (2011) 167–174.
[47] Y. Cheng, C. Yang, H. He, G. Zeng, K. Zhao, Z. Yan, Biosorption of Pb (II) ions from aqueous solutions by waste biomass from biotrickling filters: kinetics, isotherms, and thermodynamics, J. Environ. Eng., 142 (2015) C4015001.
[48] A.A. Alqadami, M. Naushad, M.A. Abdalla, M.R. Khan, Z.A. Alothman, Adsorptive removal of toxic dye using Fe_3O_4–TSC nanocomposite: equilibrium, kinetic, and thermodynamic studies, J. Chem. Eng. Data, 61 (2016) 3806–3813.
[49] E. Daneshvar, A. Vazirzadeh, A. Niazi, M. Kousha, M. Naushad, A. Bhatnagar, Desorption of Methylene blue dye from brown macroalga: effects of operating parameters, isotherm study and kinetic modeling, J. Cleaner Prod., 152 (2017) 443–453.
[50] Y. Liu, Y.-J. Liu, Biosorption isotherms, kinetics and thermodynamics, Sep. Purif. Technol., 61 (2008) 229–242.
[51] Y.C. Sharma, Effect of temperature on interfacial adsorption of Cr(VI) on wollastonite, J. Colloid Interface Sci., 233 (2001) 265–270.

[52] K.G. Bhattacharyya, S. Sen Gupta, Adsorption of chromium(VI) from water by clays, Ind. Eng. Chem. Res., 45 (2006) 7232–7240.
[53] C.-H. Weng, Y.C. Sharma, S.-H. Chu, Adsorption of Cr(VI) from aqueous solutions by spent activated clay, J. Hazard. Mater., 155 (2008) 65–75.
[54] A.K. Bhattacharya, T.K. Naiya, S.N. Mandal, S.K. Das, Adsorption, kinetics and equilibrium studies on removal of Cr(VI) from aqueous solutions using different low-cost adsorbents, Chem. Eng. J., 137 (2008) 529–541.
[55] Y. Sharma, V. Srivastava, Comparative studies of removal of Cr (VI) and Ni (II) from aqueous solutions by magnetic nanoparticles, J. Chem. Eng. Data, 56 (2010) 819–825.
[56] P. Yuan, M. Fan, D. Yang, H. He, D. Liu, A. Yuan, J. Zhu, T. Chen, Montmorillonite-supported magnetite nanoparticles for the removal of hexavalent chromium [Cr(VI)] from aqueous solutions, J. Hazard. Mater., 166 (2009) 821–829.
[57] P. Yuan, D. Liu, M. Fan, D. Yang, R. Zhu, F. Ge, J. Zhu, H. He, Removal of hexavalent chromium [Cr(VI)] from aqueous solutions by the diatomite-supported/unsupported magnetite nanoparticles, J. Hazard. Mater., 173 (2010) 614–621.
[58] H. Fida, S. Guo, G. Zhang, Preparation and characterization of bifunctional Ti–Fe kaolinite composite for Cr (VI) removal, J. Colloid Interface Sci., 442 (2015) 30–38.